Phonon-Induced Corrections to the Forbidden Hyperfine Transitions in Paramagnetic Resonance*

K. N. SHRIVASTAVA† AND JOHN E. DRUMHELLER
Department of Physics, Montana State University, Bozeman, Montana 59715
(Received 7 March 1969)

A theory for the temperature dependence of forbidden hyperfine transitions is developed within the framework of Van Vleck orbit-lattice interaction and small-wave-vector averaging procedure for acoustic phonons. Both the zero-point vibrational contribution and the temperature-dependent parts are calculated. The wave functions for the Mn^{2+} ion, calculated by Blume and Orbach to first order in the spin-orbit coupling, are used to predict the ratio of intensities of forbidden to allowed transitions for Mn^{2+} ions in octahedral crystalline fields and compared with our experimental measurements in Mn^{2+}-doped MgO. Good qualitative agreement is found, but the magnitude of temperature decrease calculated from a point-charge model is in disagreement with its experimental value.

I. INTRODUCTION

THE forbidden hyperfine transitions for which $\Delta M_s=\pm1$, $\Delta m=\pm1$, ±2, etc., occur through the mixing of neighboring hyperfine levels by off-diagonal elements in the spin Hamiltonian. Allowed transitions induced by the component of the rf magnetic field perpendicular to the axis of quantization are those for which $\Delta M_s=\pm1$, $\Delta m=0$. The parallel component of the rf field, the nuclear quadrupole interaction, and second-order cross terms between the hyperfine- and fine-structure operators in the spin Hamiltonian are known to produce forbidden hyperfine lines. The latter have been considered by Bleaney and Rubins[1] for the case of a second-order axial term in the crystalline field and by Drumheller and Rubins[2] for the cubic case. In this method, the admixtures depend on the presence of crystalline-field operators that raise or lower m by unity without affecting M_s, where m and M_s refer to the magnetic quantum number for the nuclear and electron spin, respectively. Bir[3] has shown that the direction of the effective magnetic field acting on the nuclear spin differs from the direction of the external magnetic field in the presence of crystalline field. The angle between the direction of the quantization axis and the external magnetic field depends on the orientation of the external magnetic field relative to the crystalline-field axes and also on the M_s values of the particular electron states. The dependence of the direction of the quantization axis on the electron states of the ion leads to the nonorthogonality of the nuclear-spin functions pertaining to different electronic states and corresponding to different projections of the nuclear spin. This results in the appearance of forbidden hyperfine transitions.

In all the previous studies, the crystalline field was assumed to be static. In this paper, we present the first experimental and theoretical investigation of the temperature dependence of forbidden hyperfine transitions. The lattice vibrational contribution to the intensities of forbidden transitions is calculated using Van Vleck orbit-lattice interaction.[4] The results of calculation are compared with our experimental measurements in Mn^{2+}-doped MgO single crystal.

II. THEORY

The static crystal-field interaction for an electron is usually written as an expansion in normalized spherical harmonics[5]

$$V_c=\sum_{n,m}V_n{}^m=\sum_{n,m}B_n{}^m(R)\langle r^n\rangle Y_n{}^m(\theta,\phi)\,, \qquad (1)$$

where $(r\theta\phi)$ are the coordinates of the magnetic electron, $Y_n{}^m$ are the spherical harmonics, and the factor $B_n{}^m(R)$ depends essentially on the ligands with R as the ligand coordinate. For a transition-element ion in a static (rigid-lattice) octahedral environment of ligands, the above takes the form

$$V_{\rm oct}{}^{\rm RL}=B_4(O_4{}^0+5O_4{}^4)\,, \qquad (2)$$

where B_4 is a constant, and for S-state ions, it is phenomenologically equated to $120a$, while $3a$ defines the cubic field splitting. The $O_l{}^m$ are the operator equivalents[6] having the same transformation properties as the corresponding spherical harmonics. In order to understand the resonance transitions when the external field is not parallel to the z axis, it is convenient to use states such that the electronic Zeeman terms, which are usually the biggest, are on the diagonal of the energy matrix. As pointed out by Jones *et al.*,[6] it is necessary to consider the rotation of operators $O_l{}^m$. The operators $O_l{}^{+m}$ and $O_l{}^{-m}$ do not transform in the same way upon

* Work supported by the National Science Foundation.
† Partial salary support given by the National Aeronautics and Space Administration.

[1] B. Bleaney and R. S. Rubins, Proc. Phys. Soc. (London) **77**, 103 (1961); **78**, 778 (1961).
[2] J. E. Drumheller and R. S. Rubins, Phys. Rev. **133**, A1099 (1964).
[3] G. L. Bir, Fiz. Tverd. Tela **5**, 2236 (1963) [English transl.: Soviet Phys.—Solid State **5**, 1628 (1964)].
[4] J. H. Van Vleck, J. Chem. Phys. **7**, 72 (1939); Phys. Rev. **57**, 426 (1940).
[5] B. Bleaney and K. W. H. Stevens, Rept. Progr. Phys. **16**, 108 (1953).
[6] D. A. Jones, J. M. Baker, and D. F. D. Pope, Proc. Phys. Soc. (London) **74**, 249 (1959).

rotation for arbitrary direction of the external field. It is necessary to consider all of the components of O_l^{+m} and O_l^{-m} separately and they do not have equal coefficients after rotation. When the external field is in the plane perpendicular to the z axis, this complication does not arise provided either the x or y axes of the new system of coordinates, in which the rotated operator equivalents are described, coincide with the initial z axis. Under these circumstances, we write

$$\begin{aligned} &x\rightarrow z\cos\alpha - x\sin\alpha,\\ &y\rightarrow z\sin\alpha + x\cos\alpha,\\ &z\rightarrow y. \end{aligned} \tag{3}$$

The form of (2) under the transformation (3) is

$$\begin{aligned} V_{\rm oct}^{\rm RL}(t) = B_4\{&\tfrac{3}{8}O_4^0+\tfrac{5}{2}O_4^2+(35/8)O_4^4\\ &+5[(\tfrac{1}{8}O_4^0-\tfrac{1}{2}O_4^2+\tfrac{1}{8}O_4^4)\cos 4\alpha\\ &-i(O_4^1-iO_4^3)\sin 4\alpha]\}. \end{aligned} \tag{4}$$

The neighboring hyperfine levels cannot be mixed in the first order but in second order, owing to the off-diagonal elements in the hyperfine interaction

$$\mathcal{H}_{\rm hyp} = AS_zI_z+\tfrac{1}{2}A(S_+I_-+S_-I_+). \tag{5}$$

The admixture may be written as

$$\frac{\langle M_s, m\pm1|\mathcal{H}_{\rm hyp}|M_s\pm1, m\rangle\langle M_s\pm1, m|V_{\rm oct}^{\rm RL}(t)|M_s, m\rangle}{E_{M_s,m;M_s\pm1,m}E_{M_s,m;M_s,m\pm1}}. \tag{6}$$

If only the nearest-neighbor hyperfine levels are considered, the perturbed function $|M_sm\rangle$ becomes

$$\Psi_1 = |M_s, m\rangle+\alpha|M_s, m+1\rangle+\beta|M_s, m-1\rangle. \tag{7}$$

If the allowed transition between the levels $|M_s,m\rangle$ and $|M_s-1, m\rangle$ is considered to have unit probability, then the "forbidden" transition between $|M_s, m\rangle$ and the perturbed level

$$\Psi_2 = |M_s-1, m+1\rangle+\gamma|M_s-1, m\rangle+\delta|M_s-1, m+2\rangle \tag{8}$$

must have probability

$$I_f/I_a = |\alpha+\gamma|^2, \tag{9}$$

where any of the admixture coefficients α or γ may be written explicitly as

$$\begin{aligned} \alpha=\gamma=&\frac{\langle M_s, m+1|\frac{1}{2}AS_-I_+|M_s+1, m\rangle\langle M_s+1, m|V_{\rm oct}^{\rm RL}(t)|M_s, m\rangle}{E_{M_s,m;M_s,m+1}E_{M_s,m;M_s+1,m}}\\ &+\frac{\langle M_s, m+1|V_{\rm oct}^{\rm RL}(t)|M_s-1, m+1\rangle\langle M_s-1, m+1|\frac{1}{2}AS_-I_+|M_s, m\rangle}{E_{M_s,m;M_s,m+1}E_{M_s,m;M_s-1,m+1}}. \end{aligned} \tag{10}$$

For $M_s=+(\frac{1}{2})\rightarrow-(\frac{1}{2})$ transition, the expression (9) is found[2] to be

$$\left(\frac{I_f}{I_a}\right)^2 = 25\left(\frac{B_4}{120}\right)^2\frac{I(I+1)-m(m+1)}{(g\beta H)^2}\sin^2 4\alpha. \tag{11}$$

It may be noted that the only term in $V_{\rm oct}^{\rm RL}(t)$ that has contributed to (11) is that involving the operator O_4^1, while all the other terms give zero contribution. It can now be shown how the above analysis will be influenced if the dynamic phonon interaction is taken into account.

An examination of expression (1) shows that $B_n^m(R)$ depends on ligand properties, while $\langle r^n\rangle Y_n^m(\theta\phi)$ depend exclusively on the magnetic electron. As the ligand ions undergo small oscillations about their equilibrium positions, the electrons follow the displacements in a way similar to that in dynamic Jahn-Teller effect.[7] This coupling of the electron with the lattice, which is referred to as the orbit-lattice interaction,[4,8–10] gives the thermal fluctuation in the crystalline field and may be calculated by expanding $B_n^m(R)$ in a Taylor series in terms of nuclear displacements

$$\begin{aligned} B_n^m(R) = &B_n^m(R)|_0\\ &+Q_{nm}((\partial/\partial Q_{nm})B_n^m(R))_0+\cdots. \end{aligned} \tag{12}$$

Here the Q_{nm} are linear combinations of those vibrations having the same symmetry as permitted by the magnetic electrons. The first term evaluated at equilibrium gives the usual static field while the second term gives the orbit-lattice interaction, which for an octahedral crystal with terms up to second order only, is given by[4]

$$\begin{aligned} V_{0l} = &Q_{z^2}P_{2z^2}^0+Q_{x^2-y^2}P_{2(x^2-y^2)}^2\\ &+Q_{xy}P_{2xy}^2+Q_{yz}P_{2yz}^1+Q_{zx}P_{2zx}^1, \end{aligned} \tag{13}$$

[7] M. D. Sturge, in *Solid State Physics* edited by F. Seitz, D. Turnbull, and H. Ehrenreich (Academic Press Inc., New York, 1967), Vol. 20, p. 92.

[8] R. Orbach, Proc. Roy. Soc. (London) **A264**, 458 (1961).

[9] M. Blume and R. Orbach, Phys. Rev. **127**, 1587 (1962).

[10] See also, R. Orbach and P. Pincus, Phys. Rev. **143**, 168 (1966).

where

$$
\begin{aligned}
P_{2z^2}{}^0 &= -\sum_0 A' Y_2{}^0(r_0\theta_0\phi_0)\,,\\
P_{2(x^2-y^2)^2} &= \sum_0 A'(Y_2{}^2+Y_2{}^{-2})\,,\\
P_{2xy}{}^2 &= \sum_0 A' i\tfrac{2}{3}(Y_2{}^{-2}-Y_2{}^2)\,,\\
P_{2yz}{}^1 &= \sum_0 A' i\tfrac{2}{3}(Y_2{}^1+Y_2{}^{-1})\,,\\
P_{2zx}{}^1 &= \sum_0 A' \tfrac{2}{3}(Y_2{}^1-Y_2{}^{-1})\,,
\end{aligned}
\tag{14}
$$

with

$$
A' = 9(2\pi/15)^{1/2}\frac{ee_{\text{eff}}}{R^4}\langle r^2\rangle\,, \tag{15}
$$

and the sum is over the magnetic electrons. e_{eff} is the effective charge of a ligand ion, and e is the electronic charge. The normal coordinates Q_{z^2}, etc., are the same as defined by Van Vleck. With the transformation (3), the quantities (14) are found to be

$$
\begin{aligned}
P_{2z^2}{}^0(t) &= -\tfrac{1}{2}P_{2z^2}{}^0+(\sqrt{\tfrac{3}{8}})P_{2(x^2-y^2)^2}\,,\\
P_{2(x^2-y^2)^2}(t) &= -(\sqrt{\tfrac{3}{2}})P_{2z^2}{}^0\cos 2\alpha\\
&\quad -\tfrac{1}{2}P_{2(x^2-y^2)^2}\cos 2\alpha+\tfrac{3}{2}P_{2zx}{}^1\sin 2\alpha\,,\\
P_{2xy}{}^2(t) &= -(\sqrt{\tfrac{2}{3}})P_{2z^2}{}^0\sin 2\alpha\\
&\quad -\tfrac{1}{3}P_{2(x^2-y^2)^2}\sin 2\alpha-P_{2zx}{}^1\cos 2\alpha\,,\\
P_{2yz}{}^1(t) &= P_{2yz}{}^1\sin\alpha+P_{2xy}{}^2\cos\alpha\,,\\
P_{2zx}{}^1(t) &= -P_{2yz}{}^1\cos\alpha+P_{2xy}{}^2\sin\alpha\,.
\end{aligned}
\tag{16}
$$

Following the same procedure as in the case of rigid lattice (9), the phonon-induced contribution to the ratio of intensities of forbidden to allowed transitions may be written as

$$
\left(\frac{I_f}{I_a}\right)^{\text{Phn}} = |a_1\langle M_s+1|V_{0l}(t)|M_s\rangle + a_2\langle M_s|V_{0l}(t)|M_s-1\rangle|^2\,, \tag{17}
$$

where

$$
a_1 = \frac{\langle M_s, m+1|AS_-I_+|M_s+1, m\rangle}{E_{M_s,m;M_s+1,m}E_{M_s,m;M_s,m+1}}\,, \tag{18a}
$$

$$
a_2 = \frac{\langle M_s-1, m+1|AS_-I_+|M_s, m\rangle}{E_{M_s,m;M_s-1,m+1}E_{M_s,m;M_s,m+1}}\,, \tag{18b}
$$

and the transformed orbit-lattice interaction $V_{0l}(t)$ is obtained from (13) and (16). The energy denominators in (18a) and (18b) are

$$
\begin{aligned}
E_{M_s,m;M_s+1,m} &\simeq -g\beta H\,,\\
E_{M_s,m;M_s,m+1} &\simeq AM_s\,,\\
E_{M_s,m;M_s-1,m+1} &\simeq g\beta H+AM_s\,,
\end{aligned}
\tag{19}
$$

so that for the electronic transition $M_s=+\frac{1}{2}\rightarrow -\frac{1}{2}$ with $S=\frac{5}{2}$, we have

$$
a_1 \simeq (-4\sqrt{2}/g\beta H)[I(I+1)-m(m+1)]^{1/2}\,, \tag{20a}
$$

$$
a_2 \simeq (6/g\beta H)[I(I+1)-m(m+1)]^{1/2}\,. \tag{20b}
$$

As usual, neglecting the anisotropy in the strain we find for $M_s=\frac{1}{2}$,

$$
\begin{aligned}
\left(\frac{I_f}{I_a}\right)^{\text{Phn}} &= \frac{I(I+1)-m(m+1)}{(g\beta H)^2}\{Q_{z^2}{}^2[6\langle\tfrac{1}{2}|P_{2z^2}{}^0(t)|-\tfrac{1}{2}\rangle-4\sqrt{2}\langle\tfrac{3}{2}|P_{2z^2}{}^0(t)|\tfrac{1}{2}\rangle]\\
&\quad +Q_{x^2-y^2}{}^2[6\langle\tfrac{1}{2}|P_{2(x^2-y^2)^2}(t)|-\tfrac{1}{2}\rangle-4\sqrt{2}\langle\tfrac{3}{2}|P_{2(x^2-y^2)^2}(t)|\tfrac{1}{2}\rangle]+Q_{xy}{}^2[6\langle\tfrac{1}{2}|P_{2xy}{}^2(t)|-\tfrac{1}{2}\rangle-4\sqrt{2}\langle\tfrac{3}{2}|P_{2xy}{}^2(t)|\tfrac{1}{2}\rangle]\\
&\quad +Q_{yz}{}^2[6\langle\tfrac{1}{2}|P_{2yz}{}^1(t)|-\tfrac{1}{2}\rangle-4\sqrt{2}\langle\tfrac{3}{2}|P_{2yz}{}^1(t)|\tfrac{1}{2}\rangle]+Q_{zx}{}^2[6\langle\tfrac{1}{2}|P_{2zx}{}^1(t)|-\tfrac{1}{2}\rangle-4\sqrt{2}\langle\tfrac{3}{2}|P_{2zx}{}^1(t)|\tfrac{1}{2}\rangle]\}\,,
\end{aligned}
\tag{21}
$$

where we used (17) and (20) and omitted terms involving cross products of the kind $Q_{zx}Q_{yz}$ which vanish because of orthogonality. It is now necessary to take two kinds of averages on this expression. The thermal averages are obtained from the expressions (14) and (20) of Van Vleck. The geometrical averages that are necessary to save the symmetry of the crystal as discussed by Van Vleck are found in his results (21) and (22). Taking the long-wavelength limit on acoustic phonons, we find

$$
\frac{I_f}{I_a} = \frac{I(I+1)-m(m+1)}{(g\beta H)^2}\left(25a^2\sin^2 4\alpha-\tfrac{1}{8}C\Theta^4-CT^4\int_0^{\Theta/T}\frac{x^3dx}{e^x-1}\right), \tag{22}
$$

where the first term gives the "right-lattice" contribution, the second term the zero-point phonon contribution, and the third the temperature dependence. Θ is the Debye characteristic temperature and the quantity C is given by

$$
\begin{aligned}
C &= \frac{3}{5}\frac{\hbar R^2}{\rho\pi^2}(v_l{}^{-5}+\tfrac{2}{3}v_t{}^{-5})\left(\frac{k}{\hbar}\right)^4\{6[\langle\tfrac{1}{2}|P_{2z^2}{}^0(t)|-\tfrac{1}{2}\rangle\\
&\quad +\langle\tfrac{1}{2}|P_{2(x^2-y^2)^2}(t)|-\tfrac{1}{2}\rangle+\langle\tfrac{1}{2}|P_{2xy}{}^2(t)|-\tfrac{1}{2}\rangle+\langle\tfrac{1}{2}|P_{2yz}{}^1(t)|-\tfrac{1}{2}\rangle+\langle\tfrac{1}{2}|P_{2zx}{}^1(t)|-\tfrac{1}{2}\rangle]\\
&\quad -4\sqrt{2}[\langle\tfrac{3}{2}|P_{2z^2}{}^0(t)|\tfrac{1}{2}\rangle+\langle\tfrac{3}{2}|P_{2(x^2-y^2)^2}(t)|\tfrac{1}{2}\rangle+\langle\tfrac{3}{2}|P_{2xy}{}^2(t)|\tfrac{1}{2}\rangle+\langle\tfrac{3}{2}|P_{2yz}{}^1(t)|\tfrac{1}{2}\rangle+\langle\tfrac{3}{2}|P_{2zx}{}^1(t)|\tfrac{1}{2}\rangle]\}^2\,,
\end{aligned}
\tag{23}
$$

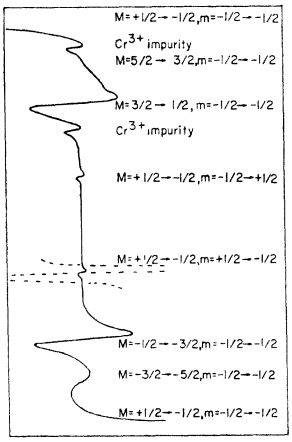

FIG. 1. Part of the spectrum of Mn^{2+}:MgO for the magnetic field making an angle of 22.5° from the cubic axis. A forbidden doublet is seen in between the allowed transitions. A particular forbidden transition (dashed line) is also shown after a magnification factor of $\simeq$100.

where v_t and v_l are the transverse and longitudinal sound velocities and ρ is the mass density of the crystal. Since the transformed operators (16) involve a rotation angle, it is important to average the quantity within curly brackets in (23) over the three principal axes of the cubic crystal so that the orbit-lattice interaction does not destroy the macroscopic cubic symmetry. Explicitly,

$$\langle \sin^2\alpha \rangle_{av} = \tfrac{2}{3}, \quad \langle \cos^2\alpha \rangle_{av} = \tfrac{1}{3}.$$

III. EXPERIMENTAL DETAILS

A high-sensitivity superheterodyne spectrometer operating at very nearly 10 GHz was modulated and phase detected at 400 Hz, resulting in a signal-to-noise ratio for the forbidden transitions of about 100:1. The single crystal of MgO had an unknown amount of manganese impurity, but the allowed and forbidden peak-to-peak derivative widths were only $\simeq$0.8 G, indicating no significant dipole-dipole broadening. The spectrometer was operated in the very low power region of $\simeq 5\,\mu$W, so as to eliminate any saturation effects in the temperature range studied. As a result, the linewidth for the allowed transitions remained constant while the linewidths for the forbidden transitions narrowed very slightly at the lowest temperatures. It is not understood whether this slight narrowing is a real or an apparent effect, however, it occurred only in a temperature region where the phonon contribution was nearly constant so that no correction is made for it.

The crystal was aligned optically and mounted in the center of a cylindrical cavity with unloaded $Q \simeq 20\,000$ operating in the TE011 mode so that the rf field was always perpendicular to the main magnetic field. Because Mn^{2+} is an S-state ion with $S=\frac{5}{2}$, $I=\frac{5}{2}$ and cubic field splitting smaller than the hyperfine splitting, the spectrum appears as six fine structure pentads with a small forbidden hyperfine doublet between each pentad. Figure 1 shows a portion of the typical spectrum between the two middle pentads for an angle of $\alpha = 22\frac{1}{2}°$ between the applied magnetic field and the ⟨100⟩ cubic axis. At each temperature, a direct comparison of the amplitudes of the allowed $(M=+\frac{1}{2} \rightarrow M=-\frac{1}{2}, m=-\frac{1}{2} \rightarrow m=-\frac{1}{2})$ transition to the forbidden $(M=+\frac{1}{2} \rightarrow M=-\frac{1}{2}, m=+\frac{1}{2} \rightarrow m=-\frac{1}{2})$ transition was made by first observing the allowed line, then the forbidden line with a gain of exactly 100. Only the one line was used consistently as Smith *et al.*[11] have shown that with no parallel component of rf, the intensities of both lines in the doublet should be equivalent. A sample of the data for two different temperatures is shown in Fig. 2. Special care was taken to keep the bridge balance exactly the same during both the absorption of the intense allowed transition and the relatively weaker forbidden transition.

IV. COMPARISON WITH EXPERIMENT

The ratio of intensities of forbidden to allowed transitions measured as a function of temperature is shown in Fig. 3. An examination of the expression (11) shows that the only way this data can depend on thermal expansion is through the cubic field splitting a. We obtained the thermal expansion contribution to a from the pressure experiments of Walsh *et al.*,[12,13] and thus corrected our intensity data for this effect. The corrected points are also shown in Fig. 3. For comparison of the theory with the experiment, we rewrite

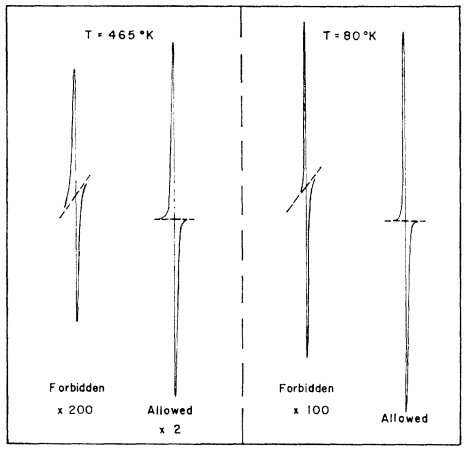

FIG. 2. Typical data for the comparison of the allowed line intensity versus the forbidden line intensity multiplied by 100, for the two temperatures (a) 80°K, (b) 465°K.

[11] S. R. P. Smith, P. V. Auzins, and J. E. Wertz, Phys. Rev. **166**, 222 (1968).
[12] W. M. Walsh, Jr., Phys. Rev. **122**, 762 (1961).
[13] W. M. Walsh, Jr., J. Jeener, and N. Bloembergen, Phys. Rev. **139**, A1338 (1965).

the expression (22) as

$$\frac{I_f}{I_a}=\left(\frac{I_f}{I_a}\right)^0-KT^4\int_0^{\Theta/T}\frac{x^3dx}{e^x-1}, \tag{24}$$

where

$$\left(\frac{I_f}{I_a}\right)^0=\frac{I(I+1)-m(m+1)}{(g\beta H)^2}[25a^2\sin^2 4\alpha-\tfrac{1}{8}C\Theta^4] \tag{25}$$

is the zero-temperature value of the intensity ratio and

$$K=C\left[\frac{I(I+1)-m(m+1)}{(g\beta H)^2}\right]. \tag{26}$$

The experimental data corrected for thermal expansion are compared with expression (24). The fit shown in Fig. 3 agrees within the experimental errors. We used the Debye temperature of 750°K for MgO as calculated by Simanek and Orbach[14] from the low-temperature specific-heat measurements of Giauque and Archibald[15] and used a numerically exact solution of the integral in (24). The parameters obtained are

$$\left(\frac{I_f}{I_a}\right)^0_{\text{expt}}=(9.01\pm0.20)\times10^{-3}, \tag{27a}$$

$$K_{\text{expt}}=(2.8\pm0.50)\times10^{-14}\ \ (°\text{K})^{-4}. \tag{27b}$$

From the second term in (25), the zero-point vibrational contribution is found to be

$$\left(\frac{I_f}{I_a}\right)^{\text{zp}}_{\text{expt}}=(1.13\pm0.20)\times10^{-3}, \tag{27c}$$

which leads to the value of the first term in (25)

$$\left(\frac{I_f}{I_a}\right)^{\text{RL}}_{\text{expt}}=(7.88\pm0.20)\times10^{-3}, \tag{27d}$$

as the "rigid-lattice" contribution to the ratio of intensities of forbidden to allowed transitions. From (27c) and (27d), we conclude that the zero-point vibrational contribution is only about 14% of the static value. Using the known[12] low-temperature value of the cubic field splitting parameter $B_4/120=a=21.45$ G and the experimental field $H=3600$ G and $I=\frac{5}{2}$, $m=-\frac{1}{2}$ and expression (11), the static intensity ratio is calculated to be

$$\left(\frac{I_f}{I_a}\right)^{\text{RL}}=7.988\times10^{-3}, \tag{28}$$

[14] E. Šimánek and R. Orbach, Phys. Rev. **145**, 191 (1966). One expression (21) is analogous to (11) of this work except for the notation. Van Vleck's Q_3 is the same as our Q_{z^2}, which is equivalent to these authors' $\frac{1}{3}R(2\epsilon_{zz}-\epsilon_{xx}-\epsilon_{yy})$.

[15] W. F. Giauque and R. C. Archibald, J. Am. Chem. Soc. **59**, 561 (1937).

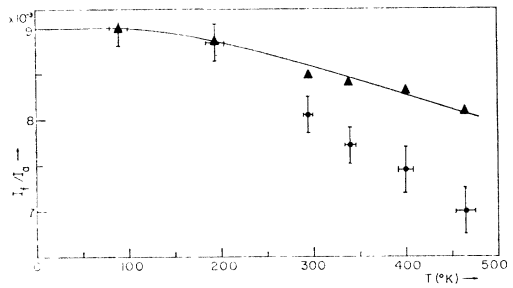

FIG. 3. Temperature dependence of the ratio of intensities of forbidden $(M=+\frac{1}{2}\rightarrow-\frac{1}{2}, m=+\frac{1}{2}\rightarrow-\frac{1}{2})$ to the allowed $(M=+\frac{1}{2}\rightarrow-\frac{1}{2}, m=\frac{1}{2}\rightarrow\frac{1}{2})$ transition of Mn^{2+} in MgO, for the magnetic field making an angle of 22.5° from a cubic axis. The triangles represent the experimental data after the correction for thermal expansion is applied and the continuous curve gives the phonon-induced shift as calculated with the data of (27a) and (27b).

which is in excellent agreement with (27d), indicating that statically the intensities are under theoretical control.

V. DIRECT COMPUTATION AND DISCUSSION OF RESULTS

In this section, we wish to obtain a purely theoretical value of the parameter K introduced in the previous section so that the calculated value may be compared with the experimental value given by (27). In the Mn^{2+} ion, the ground state is an orbital singlet so that the matrix elements of orbit-lattice interaction in (23) are all zero. However, we admix the excited states of nonvanishing orbital angular momentum into the ground state by means of spin-orbit coupling to obtain nonzero matrix elements. For reasons of selection rules in the Rusell-Saunders coupling, the strongest mixing into the ground ^6S is ^4P. The crystal field distorts several quartet states resulting in small admixtures from ^4G and ^4F as well. The wave functions, including these admixtures to first order in spin-orbit coupling as calculated by Blume and Orbach,[9,16] are

$$|{}^6SM_s\rangle'=|{}^6SM_s\rangle-\sum_{i=1}^{3}(\alpha_i\zeta/\Delta_i)[a(M_s)|{}_i{}^4\Gamma_4 1M_s-1\rangle$$
$$+b(M_s)|{}_i{}^4\Gamma_4-1,M_s+1\rangle+c(M_s)|{}_i{}^4\Gamma_4 0,M_s\rangle], \tag{29}$$

where

$$|{}_i{}^4\Gamma_4 1M_s\rangle=\{\alpha_i|P1\rangle+\beta_i[(\sqrt{\tfrac{3}{8}})|F1\rangle+(\sqrt{\tfrac{5}{8}})|F-3\rangle]$$
$$-\gamma_i[(\sqrt{\tfrac{7}{8}})|G1\rangle+(\sqrt{\tfrac{1}{8}})|G-3\rangle]\}|\tfrac{3}{2}M_s\rangle,$$
$$|{}_i{}^4\Gamma_4 0M_s\rangle=\{\alpha_i|P0\rangle+\beta_i|F0\rangle+\gamma_i[-(\sqrt{\tfrac{1}{2}})|G4\rangle$$
$$+(\sqrt{\tfrac{1}{2}})|G-4\rangle]\}\cdot|\tfrac{3}{2}M_s\rangle,$$
$$|{}_i{}^4\Gamma_4-1M_s\rangle=\{\alpha_i|P-1\rangle+\beta_i[(\sqrt{\tfrac{5}{8}})|F3\rangle+(\sqrt{\tfrac{3}{8}})|F-1\rangle]$$
$$+\gamma_i[-(\sqrt{\tfrac{3}{8}})|G3\rangle+(\sqrt{\tfrac{7}{8}})|G-1\rangle]\}|\tfrac{3}{2}M_s\rangle.$$

[16] See also, R. R. Sharma, T. P. Das, and R. Orbach, Phys. Rev. **149**, 257 (1966); **171**, 378 (1968).

TABLE I. The spin-orbit admixture coefficients of excited cubic field states into the ground state of the Mn^{2+} ion.

M_s	$\frac{5}{2}$	$\frac{3}{2}$	$\frac{1}{2}$	$-\frac{1}{2}$	$-\frac{3}{2}$	$-\frac{5}{2}$
$a(M_s)$	$+\sqrt{5}$	$+\sqrt{3}$	$+\frac{1}{2}\sqrt{6}$	$+\frac{1}{2}\sqrt{2}$	0	0
$b(M_s)$	0	0	$+\frac{1}{2}\sqrt{2}$	$+\frac{1}{2}\sqrt{6}$	$+\sqrt{3}$	$+\sqrt{5}$
$c(M_s)$	0	$-\sqrt{2}$	$+\sqrt{3}$	$+\sqrt{3}$	$+\sqrt{2}$	0

$a(M_s)$, $b(M_s)$, and $c(M_s)$ are defined by

$$a(M_s)=\tfrac{1}{2}\langle {}^4P1M_s-1|\sum_j l_j^+ s_j^-|{}^6SM_s\rangle,$$
$$b(M_s)=\tfrac{1}{2}\langle {}^4P-1M_s+1|\sum_j l_j^- s_j^+|{}^6SM_s\rangle, \quad (30)$$
$$c(M_s)=\langle {}^4P0M_s|\sum_j l_j^z s_j^z|{}^6SM_s\rangle,$$

and $|{}^4PM_LM_S\rangle=|{}^4PM_L\rangle|SM_S\rangle$. The quantities (30) are given in Table I. The matrix elements of $P_i(t)$ in (23) are calculated using the wave functions of (29) and the usual formula[9]

$$\langle l^n\alpha'SL'M_sM_L'|\sum_i Y_\lambda^\mu(i)|l^n\alpha SLM_sM_L\rangle$$
$$=(-1)^{L'-M_L'}\begin{pmatrix} L' & \lambda & L \\ -M_L' & \mu & M_L\end{pmatrix}\times\langle l^n\alpha'SL'||\sum_i Y_\lambda(i)||l^n\alpha SL\rangle, \quad (31)$$

with

$$\langle l^n\alpha'SL'||\sum_i Y_\lambda(i)||l^n\alpha SL\rangle$$
$$=\left(\frac{2\lambda+1}{4\pi}\right)^{1/2} n(2l+1)[(2L+1)(2L'+1)]^{1/2}\times\begin{pmatrix} l & \lambda & l \\ 0 & 0 & 0\end{pmatrix}\sum_{\alpha_1S_1L_1}(-1)^{L+L_1}\langle l^n\alpha'SL'\times(|l^{n-1}\alpha_1L_1S_1\rangle\langle l^{n-1}\alpha_1S_1L_1|)\times l^n\alpha SL\rangle\begin{Bmatrix} L & \lambda & L' \\ l & L_1 & l\end{Bmatrix}, \quad (32)$$

where the three- and six-j symbols are tabulated by Rotenberg, *et al.*,[17] and the fractional parentage coefficients are given by Racah.[18] Using $v_t=6.3\times10^5$ cm/sec, $v_l=8.8\times10^5$ cm/sec, $R=2.1\times10^{-8}$ cm, $\rho=3.7$ g/cc, $e_{\text{eff}}=2e$, appropriate[19] to MgO and $\langle r^2\rangle=1.548a_0^2$, $\zeta=300$ cm^{-1}, and $D_q=900$ cm^{-1} for Mn^{2+}, and the experimental field $H=3600$ G, we calculate

$$K_{\text{cal}}=1.22\times10^{-13}\ (^\circ\text{K})^{-4}. \quad (33)$$

This is to be compared to the experimental value (27b) of 2.8×10^{-14} $(^\circ\text{K})^{-4}$. The calculated value is an order of magnitude higher than the measured one. Part of the discrepancy may be due to uncertainties in several parameters involved in the calculation. Errors would also arise because of the use of the Debye model for lattice vibrations which is not strictly valid.

In conclusion, we have shown that a part of temperature dependence in the forbidden intensities arises from thermal expansion and a significant part from lattice vibrations. The calculated strength of variation of the phonon induced contributions is somewhat in disagreement with the experiment in Mn^{2+}-doped MgO, but this discrepancy may be due to uncertainties in the parameters involved or possibly because of neglect of any covalent contributions.

ACKNOWLEDGMENTS

The authors wish to thank Professor R. Orbach for helpful discussions and D. H. Dickey for his assistance with the experimental apparatus.

[17] M. Rotenberg, R. Bivins, N. Metropolis, and J. K. Wooten, Jr., *The 3-j and 6-j Symbols* (MIT Press, Cambridge, Massachusetts, 1959).

[18] G. Racah, Phys. Rev. **63**, 367 (1943).

[19] H. B. Huntington, in *Solid State Physics* edited by F. Seitz and D. Turnbull (Academic Press Inc., New York, 1958), Vol. 7, p. 214.